

# Collective chaos in pulse-coupled neural networks

SIMONA OLMI<sup>1,2,3</sup>, ANTONIO POLITI<sup>1,3</sup> and ALESSANDRO TORCINI<sup>1,2,3</sup>

<sup>1</sup> *Istituto dei Sistemi Complessi, CNR, via Madonna del Piano 10, I-50019 Sesto Fiorentino, Italy*

<sup>2</sup> *INFN Sez. Firenze, via Sansone, 1 - I-50019 Sesto Fiorentino, Italy*

<sup>3</sup> *Centro Interdipartimentale per lo Studio delle Dinamiche Complesse, via Sansone, 1 - I-50019 Sesto Fiorentino, Italy*

PACS 05.45.-a – Nonlinear dynamics and chaos  
 PACS 05.45.Xt – Synchronization; coupled oscillators  
 PACS 84.35.+i – Neural networks  
 PACS 87.19.1j – Neuronal network dynamics

**Abstract.** - We study the dynamics of two symmetrically coupled populations of **identical** leaky integrate-and-fire neurons characterized by an excitatory coupling. Upon varying the coupling strength, we find symmetry-breaking transitions that lead to the onset of various chimera states as well as to a new regime, where the two populations are characterized by a different degree of synchronization. Symmetric collective states of increasing dynamical complexity are also observed. The computation of the the finite-amplitude Lyapunov exponent allows us to establish the chaoticity of the (collective) dynamics in a finite region of the phase plane. The further numerical study of the standard Lyapunov spectrum reveals the presence of several positive exponents, indicating that the microscopic dynamics is high-dimensional.

**Introduction.** – Understanding the collective motion of ensembles/networks of oscillators is crucial in many contexts, starting from neuronal circuits [1]. So far, most of the efforts have been devoted to the characterization of strong forms of synchronization. However, more subtle phenomena, like the onset of collective motion in an ensemble of (chaotic) units, which behave in a seemingly uncorrelated way can also play a relevant role for information encoding. Collective chaos, meant as irregular dynamics of coarse-grained observables, has been found in ensembles of fully coupled one-dimensional maps [2,3] as well as in two-dimensional continuous-time oscillators [4–6]. In both classes of models, the single dynamical unit can behave chaotically under the action of a periodic forcing (in non-invertible maps, there is even no need of a periodic forcing). What does it happen in ensembles of phase-oscillators which cannot become chaotic under the action of any forcing? The evolution of a (formally infinite) population of oscillators is ruled by a self-consistent (nonlinear) functional equation for the probability density. Given the infinite dimensionality of the model, the population could, in principle, behave chaotically, irrespective of the “structure” of the single oscillators. In spite of this potentiality, **only a few examples of low-dimensional** chaotic collective motion **have** been found in ensembles of phase-oscillators

[7,8]. One reason is that most of the models so far investigated are based on sinusoidal force fields (in the following we refer to them as to sinusoidal oscillators); in this setup, there is little space for a high dimensional dynamics, since no matter how many oscillators are involved, there are always  $N - 3$  constants of motion [8]. This “degeneracy” is not present in typical pulse-coupled networks of neurons, where different force fields are usually assumed. A prototypical example is that of leaky integrate-and-fire (LIF) neurons, characterized by a linear force field. It is, in fact, not surprising that the first instance of a non-trivial collective motion has been found in an ensemble of LIF neurons. We refer to Partial Synchronization (PS) [9], a regime characterized by a periodic macroscopic dynamics and a quasiperiodic microscopic motion, with the additional subtlety that the average inter-spike interval of the single neurons differs from the period of the collective variable. More recently, this type of behaviour has been observed also in a population of sinusoidal oscillators, in the presence of a suitable nonlinear coupling [10].

The only and quite striking evidence of an irregular collective dynamics has been recently found in an ensemble of LIF neurons in the presence of a random distribution of the input currents [11] (this setup, where the single neurons are characterized by different spiking rates, is anal-

ogous to that of the usual Kuramoto model, where the single oscillators have different bare frequencies). On the other hand, the model studied in [11] has the further peculiarity of exhibiting a negative maximal Lyapunov exponent – it is, in fact, an example of *stable chaos* [12]. However, in the absence of disorder, no example of irregular dynamics has yet been found.

A slightly more complex but meaningful setup is that of two symmetrically coupled populations of identical oscillators. This is the simplest instance of “network-of-networks” that is often invoked as a paradigm for neural systems [13]. With reference to sinusoidal oscillators, this setup has revealed the onset of chimera states (one of the two populations is fully synchronized, while the oscillators of the other one are not synchronized at all [14]), as well as more complex macroscopic states with periodic [15] and quasi-periodic [16] collective oscillations. In the present Letter we study the two-population setup with reference to LIF neurons for different values of the coupling strengths between and within the two populations. We find various kinds of symmetry broken states some of which are similar to those observed in [15, 16] and a new one, where the two populations are both partially synchronized, but with a different degree. More interesting is the parameter region where the collective motion is chaotic, as indicated by the finite-amplitude Lyapunov exponent (FALE) [17] and confirmed by the computation of the standard Lyapunov spectrum which reveals the existence of several positive exponents.

**The model.** – We consider two fully coupled networks, each made of  $N$  LIF oscillators. Following Refs. [18], the membrane potential  $x_j^{(k)}(t)$  of the  $j$ -th oscillator ( $j = 1, \dots, N$ ) of the  $k$ th population ( $k = 0, 1$ ) evolves according to the differential equation,

$$\dot{x}_j^{(k)}(t) = a - x_j^{(k)}(t) + g_s E^{(k)}(t) + g_c E^{(1-k)}(t) \quad (1)$$

where  $a > 1$  is the suprathreshold input current, while  $g_s > 0$  and  $g_c > 0$  gauge the self- and, resp., cross-coupling strength of the excitatory interaction. **Whenever the membrane potential reaches the threshold  $x_j^{(k)} = 1$ , it is reset to  $x_j^{(k)} = 0$ , while a so-called  $\alpha$ -pulse is sent and instantaneously received by all the neurons. The field  $E^{(k)}(t)$  represents the linear superposition of the pulses emitted within the population  $k$  in the past. It can be shown [18] that  $E^{(k)}(t)$  satisfies the differential equation**

$$\ddot{E}^{(k)}(t) + 2\alpha\dot{E}^{(k)}(t) + \alpha^2 E^{(k)}(t) = \frac{\alpha^2}{N} \sum_{j,n} \delta(t - t_{j,n}^{(k)}), \quad (2)$$

where  $t_{j,n}^{(k)}$  is the  $n$ th spiking time of the  $j$ th neuron within the population  $k$ , and the sum is restricted to times smaller than  $t$ . In the limit case  $g_s = g_c = g$ , the two populations can be seen as a single one made of  $2N$  neurons with an effective coupling constant  $G = 2g$ .

The degree of synchronization can be quantified by introducing the typical order parameter used for phase

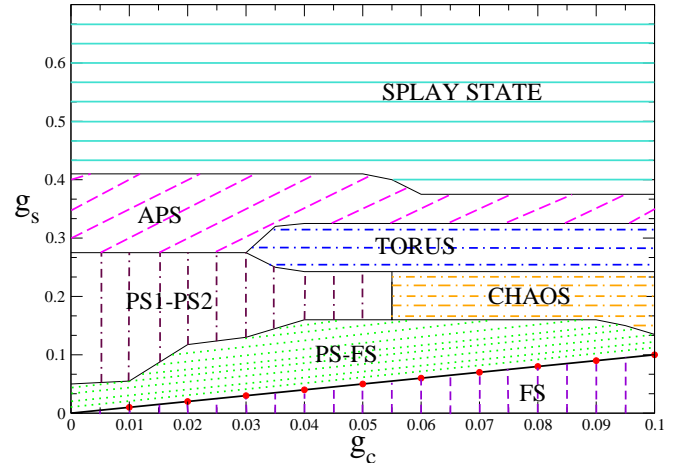


Fig. 1: (Color Online) Phase diagram in the  $(g_c, g_s)$ -plane of the model (1,2) for  $a = 1.3$  and  $\alpha = 9$ . FS indicates Full Synchronization (both populations fire at the same time); PS-FS indicates that the two populations are in the FS and PS regimes, respectively; PS1-PS2 indicates that both populations are in a PS regime, although with a different degree of synchronization; APS indicates Antiphase Partial Synchronization, i.e. the two fields exhibit the same behaviour though being in antiphase; TORUS indicates a collective quasi-periodic motion; finally, CHAOS indicates collective chaotic motion.

oscillators  $r^{(k)}(t) = \left| \langle \exp[i\theta_j^{(k)}(t)] \rangle \right|$ , where  $\theta_j^{(k)}$  is the phase of the  $j$ th oscillator, that can be properly defined by suitably rescaling the time variable [19],  $\theta_j^{(k)}(t) = 2\pi(t - t_{j,n}^{(k)}) / (t_{q,n}^{(k)} - t_{q,n-1}^{(k)})$ , where  $n$  identifies the last spike emitted by the  $j$ th neuron, while  $q$  indicates the neuron that has emitted the last spike. One can verify that this phase is bounded between 0 and  $2\pi$ , as it should. It is interesting to see that the application of this definition to the PS regime described by van Vreeswijk [9] reveals that the order parameter fluctuates periodically. In other words PS differs from the regime observed in the Kuramoto model above the synchronization threshold, where the order parameter is constant in time [20].

**Phase Diagram.** – The equations have been integrated by extending the event-driven approach described e.g. in [18]. In practice, the (linear) equations of motion are solved analytically in between two consecutive spike-emissions, obtaining a suitable map. Since the ordering of the single-neuron potentials does not change within each population, the next firing event can be easily determined by comparing the neurons that are closest to threshold within each of two populations. In spite of the conceptual simplicity and the effectiveness of the code, one must be nevertheless careful in handling nearly singular cases, when many neurons almost cluster together. In order to avoid the spurious clustering, due to numerical roundoff, we have changed variables, introducing and monitoring the logarithm of the difference of the membrane potentials of two successive neurons. This requires some care

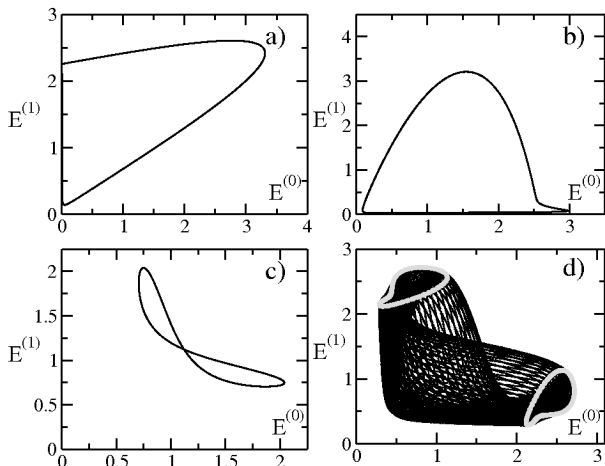


Fig. 2: The macroscopic attractors displayed by reporting the fields  $E^{(0)}$  vs  $E^{(1)}$  for four different non chaotic phases, namely (a) PS-FS ( $g_c = 0.07$ ,  $g_s = 0.1$ ), (b) PS1-PS2 ( $g_c = 0.02$ ,  $g_s = 0.17$ ), (c) APS ( $g_c = 0.07$ ,  $g_s = 0.35$ ) and (d) TORUS ( $g_c = 0.07$ ,  $g_s = 0.3$ ) (for the exact definitions see the text). The **grey** curves reported in the panel (d) are the Poincaré sections obtained by imposing that the sum  $E^{(0)} + E^{(1)}$  is maximal.

in defining the right number of variables: given  $N$  potentials, one naturally has  $N - 1$  differences that have to be complemented by a proper  $N$ th variable (for more details see [21]).

The phase plane ( $g_c, g_s$ ) shown in Fig. 1 has been obtained by studying the model (1,2) for  $a = 1.3$  and  $\alpha = 9$ . The diagram is semiquantitative in the sense that a much more detailed work would be needed to identify exactly the stability borders of the different regimes. Along the diagonal ( $g = g_s = g_c$ ) the model reduces to that for a single population with coupling strength  $G = 2g$ . For our choice of  $a$  and  $\alpha$  values, the system exhibits PS, since we are below the critical value  $G_0 = 0.425$  [18] above which the splay state is stable (the splay state is a regime characterized by a constant spiking rate and thereby a constant field, i.e. no collective dynamics). Below the diagonal, the evolution is still symmetric but fully synchronized (FS), i.e. all neurons of both populations fire together. More intriguing is the region above the diagonal, that is characterized by a spontaneous symmetry breaking: one population fully synchronizes, while the other is in a PS regime, i.e. we are in presence of a generalized chimera state (here termed PS-FS). This can be appreciated by looking at the synchronization parameter  $r^{(k)}$  of the two populations, one of which is equal to one, while the other oscillates periodically close to 0.8. By following [15], this state can be classified as a *periodically breathing chimera*. In this regime, the two populations are characterized by a microscopically periodic and quasi-periodic behaviour, respectively. In spite of this qualitative difference, the two (macroscopic) fields  $E^{(0)}$  and  $E^{(1)}$  are both periodic and phase locked (see Fig. 2a). This means that the neurons subject to two different linear combinations of  $E^{(0)}$  and  $E^{(1)}$  behave dif-

ferently: a population locks with the forcing field, while the other one behaves quasi-periodically. Another even more interesting symmetry broken state can be observed for larger  $g_s$ -values and  $g_c < 0.055$ ; in this case both populations exhibit PS, but their dynamics take place over two different attractors with two different degrees of synchronization (PS1-PS2 regime), as shown in Fig. 3a. Like in the PS-FS regime, the two fields behave periodically (with the same period) and are phase locked, as it can be appreciated by looking at the closed curve  $E^{(0)}$  versus  $E^{(1)}$  in Fig. 2b. However, at variance with PS-FS, here both populations exhibit quasi-periodic motions. In other words we are in presence of a different symmetry breaking, where two populations with distinct quasi-periodic motions spontaneously emerge. For yet larger  $g_s$  values, the equivalence between the collective dynamics of the two population is restored, the only difference being a phase shift between the two fields, which oscillate in antiphase and this is why we term this regime *Antiphase Partial Synchronization* (APS). In the APS phase, for finite  $N$ , the **instantaneous** maximum Lyapunov exponent strongly fluctuates and we cannot rule out the possible existence of some form of weak chaos, analogous to the one discussed in [22] for a model of diluted neural network, i.e. a chaotic behaviour that disappears in the thermodynamic limit. In a strip above the chaotic region (discussed below), one can observe collective quasiperiodic motion. This means that the quasiperiodic motion of the fields is accompanied by a dynamics of the single neurons along a torus  $T^3$ . An analogous regime has been previously reported in [5] in the context of a population of coupled Stuart-Landau oscillators. Here, we find it in a model where the single units are described by a single variable. Furthermore, we have characterized the motion on the macroscopic  $T^2$  attractor reported in Fig. 2, by estimating the winding numbers for various values of the coupling strengths. We find that the winding number is typically quite small – on the order of  $\sim 10^{-2}$  – but independent of the system size, indicating that the torus survives in the thermodynamic limit. Finally, for yet larger  $g_s$ -values both populations converge towards a splay state. This is not surprising, as we already know that for the chosen  $\alpha$ - and  $a$ -values, the splay state is stable in a single population of neurons for  $G > G_0 \equiv 0.425$ .

**Collective Chaos.** – In a limited region above the diagonal and for  $g_c > 0.055$  the collective behaviour is irregular, this is clearly seen by observing the two macroscopic attractors, corresponding to the two populations, reported in Fig. 3b. Nonetheless, from Fig. 3c it appears that the associated order parameters behave almost periodically, but this periodicity is only apparent since it reflects only the larger time scale present in the system, the one associated to the modulation of the fields  $E^{(k)}$ , while the irregularity of the dynamics are more evident at smaller time scales. In particular, **at least two other** time scales are present: a scale  $\mathcal{O}(1)$  associated to the

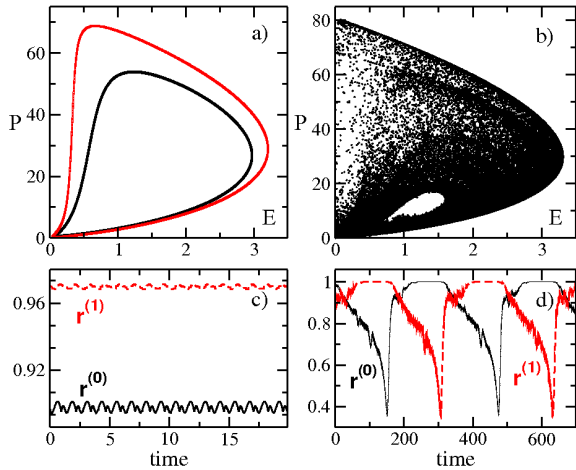


Fig. 3: (Color Online) Macroscopic attractors displayed by reporting  $P \equiv E + \alpha \dot{E}$  vs  $E$  for a PS1-PS2 state (a) and a chaotic phase (b), the time evolution of the corresponding order parameters  $r^{(0)}$  and  $r^{(1)}$  is also reported in (c) and (d). The variables corresponding to population 0 (resp. 1) are shown as black solid lines (resp. red dashed lines) in (c) and (d); while in (a) the internal black (resp. external red) curve refers to population 0 (resp. 1) and in (b) a unique attractor has been reported for clarity reasons, since the two attractors are overlapping. The data reported in (a) and (c) refer to  $g_c = 0.02$  and  $g_s = 0.17$ , while those shown in (b),(d) to  $g_c = 0.08$  and  $g_s = 0.16$ .

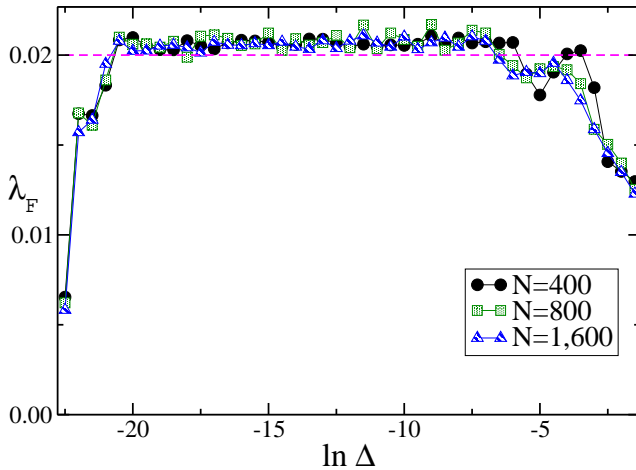


Fig. 4: Finite amplitude Lyapunov exponents  $\lambda_F$  versus the logarithm of the perturbation amplitude  $\Delta$  for three different system sizes: namely,  $N = 400$  (black circles),  $N = 800$  (green squares) and  $N = 1,600$  (blue triangles). The amplitudes  $\Delta$  have been estimated by considering the euclidean distance among the perturbed and unperturbed fields. The dashed (magenta) line indicates the maximal microscopic Lyapunov exponent  $\lambda_1$  for  $N = 1,600$  obtained by following the orbit over a time span containing  $10^8$  spikes and after discarding a transient composed by  $10^6$  spikes.  $\lambda_F$  has been estimated by averaging over 25,000 – 50,000 different trajectories. The results have been obtained for  $g_c = 0.08$  and  $g_s = 0.16$ .

firing period of each specific neuron and a scale  $\mathcal{O}(1/N)$  corresponding to the interspike interval between two successive spike emissions in the network. In order to make a quantitative assessment of the chaoticity we have first studied the FALE  $\lambda_F$ . The FALE can be determined from the growth rate of a small finite perturbation for different amplitudes  $\Delta$  of the perturbation itself (after averaging over different trajectories) [17]. This is done by randomly perturbing the coordinates (both fields and the membrane potentials of the two populations) of a generic configuration on the attractor. The results for  $g_s = 0.16$ ,  $g_c = 0.08$  and three different system sizes are plotted in Fig. 4. For small  $\Delta$  values,  $\lambda_F$  grows with  $\Delta$ , since the perturbation needs first to converge towards the most expanding direction, while the final drop is a manifestation of the saturation of the perturbation amplitude. It is the height of the intermediate plateau which measures the amplitude of the FALE. Since the height is independent of  $N$ , one can conjecture that the collective motion is chaotic and stays chaotic in the thermodynamic limit. Besides the data reported in Fig. 4, we have checked that the plateau height is not influenced by changing the amplitude of the initial perturbation and by performing tests up to  $N=6,400$ .

It is instructive to compare  $\lambda_F$  with the maximum  $\lambda_1$  of the standard Lyapunov spectrum. For small  $\Delta$  values, the two indicators should coincide, but there is no reason for the agreement to persist at larger amplitudes. In fact, a second plateau has been detected in the context of globally coupled maps [2, 3]. The plateau occurring for larger  $\Delta$ 's has been interpreted as an indication that the chaoticity of collective variables differs from that of the microscopic ones. Since, in the present case, we observe only a single plateau, it is crucial to verify its compatibility with  $\lambda_1$ . The horizontal dashed line in Fig. 4 corresponds to the Lyapunov exponent determined for  $N=1,600$  (for the dependence of  $\lambda_1$  on  $N$ , see below). The two indicators are consistent with each other and this means that collective variables are as chaotic as the microscopic ones.

Having established the existence of one unstable direction, the next question is to determine how many such directions are present. Unfortunately, the concept of FALE allows to determine just one exponent. As a consequence, we turn our attention to the usual Lyapunov spectrum, well aware that the “microscopic” exponents do not necessarily reproduce the chaoticity of the “macroscopic” variables.

In the present model, the Lyapunov spectrum  $\{\lambda_i\}$  is composed of  $N + 3$  exponents ( $i = 1, \dots, N + 3$ ). The phase space dimension is in fact equal to  $N + 4$  ( $N$  potentials plus 2 two-dimensional equations for the fields), but the direction corresponding to the zero-Lyapunov exponent is implicitly eliminated as a consequence of taking the Poincaré section [18]. In Fig. 5 we have plotted the first part of the spectrum (with the exception of  $\lambda_1$ , for the clarity of presentation) with the usual normalization  $i/N$  of the  $x$  axis. The figure clearly indicates that the spectrum becomes increasingly flat and converges to zero. This

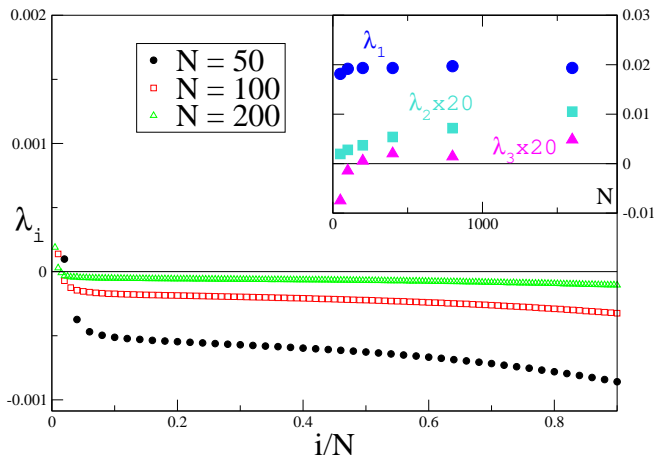


Fig. 5: (Color Online) Lyapunov spectra  $\lambda_i$  versus  $i/N$  for three  $N$ -values: namely,  $N = 50$  (filled black circles),  $N = 100$  (empty red squares) and  $N = 200$  (empty green triangles). In the inset the first three Lyapunov exponents are reported as a function of  $N$ :  $\lambda_1$  (blue circles),  $\lambda_2$  (turquoise squares) and  $\lambda_3$  (magenta triangles). The Lyapunov exponents have been obtained by following the dynamics in the real and tangent space for a time span containing  $10^8 - 5 \times 10^9$  spikes, after discarding a transient period of  $10^6$  spikes. The reported results refer to  $g_c = 0.08$  and  $g_s = 0.16$ .

can be understood in the following way. In the thermodynamic limit, the dynamics of globally coupled identical oscillators can be viewed as that of single oscillators forced by the same (self-consistent) field [5]. As a result, in a first approximation, we expect all Lyapunov exponents to be equal to the conditional Lyapunov exponent  $\lambda_c$  obtained by forcing a single LIF neuron (identical to the others) with the self-consistent fields (obtained by integrating the whole ensemble). We have found that  $\lambda_c = 0$  (within numerical accuracy). This justifies why the increasingly flat Lyapunov spectrum converges towards zero. Moreover, since a LIF neuron is described by a single variable, under no circumstance,  $\lambda_c$  can be strictly positive. On the other hand,  $\lambda_c$  can be negative, and we expect this to occur whenever the given population exhibits full synchronization. Since we know that no synchronization is observed in the chaotic regime, we can conclude that  $\lambda_c$  is not just very small, but it must be exactly equal to zero.

Having established that the Lyapunov spectrum converges to zero, it is interesting to investigate its scaling behaviour. By comparing the spectra obtained for different system sizes, it turns out that they scale as  $1/N^\beta$ , although we are unable to extrapolate the value of  $\beta$  from the analysis of the relatively small systems that we have simulated. By comparing the spectra obtained for  $N = 100$  and  $200$  we can at most guess that  $\beta \approx 1.5$ . This value is not far from  $\beta = 2$ , found analytically while studying the splay-state stability in single populations of LIF neurons [23] and numerically for the PS state [22].

Finally, we turn our attention to the first part of the spectrum, where the flatness hypothesis does not hold.

More precisely, we investigate the  $N$ -dependence of the first three Lyapunov exponents which can be computed for larger lattices (up to  $N=1,600$ ). The maximal Lyapunov exponent appears to converge to a finite asymptotic value  $\lambda_1 = 0.0195(3)$ . On the other hand, the second and third exponents grow systematically with  $N$ , both becoming positive for  $N > 200$ , with no clear evidence of an eventual saturation. These results suggest that the microscopic chaos is high-dimensional (there is no reason to believe that the number of positive exponents is just equal to three). However, we cannot tell whether the number of positive exponents is extensive (proportional to  $N$ ) or sub-extensive.

**Conclusions.** – We have studied two symmetrically coupled populations of leaky integrate-and-fire neurons for different values of the self- ( $g_s$ ) and cross- ( $g_c$ ) coupling-strength. Some of the collective phenomena that we have identified are quite similar to those observed in the two-population setup of Kuramoto-like oscillators [24]. This is not surprising, since it is known that an ensemble of LIF neurons is equivalent, in the weak coupling limit, to the Kuramoto model [25], the only difference being that the coupling function is not purely sinusoidal. The onset of PS in both classes of models suggests that the equivalence can be extended to larger coupling strengths. However, since PS can be obtained in the Kuramoto setup only by invoking a more general kind of coupling [10], it is legitimate to conclude that the relationship is more complicated than that suggested by the study of the weak-coupling limit. In fact, in this Letter we have found new dynamical regimes, such as a different PS dynamics for the two populations. A yet more intriguing phenomenon is the collective chaos that we have recognized as such from the computation of the finite-amplitude Lyapunov exponent. Altogether, a general question still stands: **To what extent are pulse-coupled oscillators** equivalent to Kuramoto-like models? The identification of the mutual relationship would be highly beneficial in both areas.

Another still open question is that of the degree of chaoticity of the collective dynamics. This problem is also connected to that of the asymptotic structure of the Lyapunov spectrum in the thermodynamic limit. A rough argument suggests that the spectrum should be flat and this is indeed approximately seen in the numerics. However, the evident deviations observed in the vicinity of the maximum strongly suggest that the argument need be refined. Altogether, we observe that the Lyapunov spectrum includes the FALE. This means that the evolution of not-so-small perturbations does not add anything, to that of infinitesimal ones and implies that the standard Lyapunov analysis is rich enough to account for the collective behaviour as well. This was not a priori obvious. The computation of the FALE  $\lambda_F$  in globally coupled maps [3] reveals a different scenario, where  $\lambda_F$  differs from the maximum Lyapunov exponent. On the other hand, the more recent study of globally coupled Stuart-Landau oscillators

[26] provides an example where, like here, the chaoticity of the collective motion can be inferred from the Lyapunov spectrum. Moreover, what can we say about the role of the second and third exponents that are found to be positive as well? Do they contribute to the microscopic dynamics only, or also to the macroscopic one? A careful analysis based on the study of the corresponding covariant Lyapunov vectors [27] might help to clarify this point. An alternative and more direct approach could be that of (numerically) integrating the self-consistent dynamical equation for the probability densities of the membrane potentials in the two families. However, it is not easy to pursue this latter perspective: because of the occasional formation of strongly clusterized states, it is necessary to partition the phase space into a huge number of small cells.

\* \* \*

We thank M. Cencini, F. Ginelli, A. Pikovsky and S.H. Strogatz for a careful reading of the manuscript. This research project is part of the activity of the Joint Italian-Israeli Laboratory on Neuroscience funded by the Italian Ministry of Foreign Affairs and it has been partially realized thanks to the support of CINECA through the Italian Super Computing Resource Allocation (ISCRA) programme, project ECOSFNN.

## REFERENCES

- [1] BUZSÁKI G., *Rhythms of the Brain* (Oxford University Press, Oxford) 2006
- [2] SHIBATA T. and KANEKO K., *Phys. Rev. Lett.*, **81** (1998) 4116.
- [3] CENCINI M., FALCIONI M., VERGNI D. and VULPIANI A., *Physica*, **130D** (1999) 58.
- [4] MATTHEWS P.C., MIROLLO R.E. and STROGATZ S.H., *Physica*, **52D** (1991) 293.
- [5] NAKAGAWA N. and KURAMOTO Y., *Physica*, **80D** (1995) 307.
- [6] HAKIM V. and RAPPEL W-J., *Phys. Rev. A*, **46** (1992) R7347.
- [7] GOLOMB D., HANSEL D., SHRAIMAN B., and SOMPOLINSKY H., *Phys. Rev. A*, **45** (1992) 3516; MARVEL S.A., MIROLLO R.E. V. and STROGATZ S.H., *Chaos*, **19** (2009) 043104.
- [8] WATANABE S. and STROGATZ S.H., *Phys. Rev. Lett.*, **70** (1993) 2391.
- [9] VAN VREESWIJK C., *Phys. Rev. E*, **54** (1996) 5522.
- [10] ROSENBLUM M. and PIKOVSKY A., *Phys. Rev. Lett.*, **98** (2007) 064101.
- [11] LUCCIOLI S. and POLITI A., *Phys. Rev. Lett.*, **105** (2010) 158104
- [12] POLITI A. and TORCINI A., *Nonlinear Dynamics and Chaos: Advances and Perspectives*, edited by THIEL, M., KURTHS, J., ROMANO, M.C., MOURA, A. and KÁROLYI, G. (Springer Verlag, Heidelberg) 2010, p. 103.
- [13] MONTBRIÓ E., KURTHS J., and BLASIUS B., *Phys. Rev. E*, **70** (2004) 056125; BARRETO E., HUNT B., OTT. E. and SO P., *Phys. Rev. E*, **77** (2008) 036107.
- [14] ABRAMS D.M. and STROGATZ S.H., *Phys. Rev. Lett.*, **93** (2004) 174102.
- [15] ABRAMS D.M., MIROLLO R.E., STROGATZ S.H. and WILEY D.A., *Phys. Rev. Lett.*, **101** (2008) 084103.
- [16] PIKOVSKY A. and ROSENBLUM M., *Phys. Rev. Lett.*, **101** (2008) 264103.
- [17] AURELL E., BOFFETTA G., CRISANTI A., PALADIN G. and VULPIANI A., *Phys. Rev. Lett.*, **77** (1996) 1262.
- [18] ZILLMER R., LIVI R., POLITI A. and TORCINI A., *Phys. Rev. E*, **76** (2007) 046102.
- [19] WINFREE A.T., *The Geometry of Biological Time* (Springer Verlag, Berlin) 1980.
- [20] KURAMOTO Y., *Chemical Oscillations, Waves, and Turbulence* (Dover Publications) 2003.
- [21] OLM S., POLITI A. and TORCINI A., *in preparation*, ()
- [22] OLM S., LIVI R., POLITI A. and TORCINI A., *Phys. Rev. E*, **81** (2010) 046119.
- [23] CALAMAI M., POLITI A. and TORCINI A., *Phys. Rev. E*, **80** (2009) 036209.
- [24] By Kuramoto-like we mean sinusoidal oscillators with some sort of continuous-time coupling that depends on the phase-differences.
- [25] HANSEL D., MATO G. and MEUNIER C., *Neural Comput.*, **7** (1995) 307.
- [26] TAKEUCHI K.A., GINELLI F. and CHATÉ H., *Phys. Rev. Lett.*, **103** (2009) 154103.
- [27] GINELLI F., POGGI P., TURCHI A., CHATÉ H., LIVI R. and POLITI A., *Phys. Rev. Lett.*, **99** (2007) 130601.